REPORT DOCUMENTATION PAGE

Form Approved
OMB No. 0704-0188

1. REPORT DATE *(DD-MM-YYYY)*	2. REPORT TYPE	3. DATES COVERED *(From - To)*
19-02-2008	Journal Article	

4. TITLE AND SUBTITLE

A Numerical Approach to Solving the Hall MHD Equations Including Diamagnetic Drift (Preprint)

5a. CONTRACT NUMBER
FA9300-06-D-0002 0003

5b. GRANT NUMBER

5c. PROGRAM ELEMENT NUMBER

6. AUTHOR(S)
John Loverich (Advatech Pacific); Jean-Luc Cambier (AFRL/RZSA)

5d. PROJECT NUMBER

5e. TASK NUMBER
5026SBM3

5f. WORK UNIT NUMBER

7. PERFORMING ORGANIZATION NAME(S) AND ADDRESS(ES)

Advatech Pacific
950 E. Palmdale Boulevard, Suite C
Palmdale CA 93550

8. PERFORMING ORGANIZATION REPORT NUMBER

AFRL-RZ-ED-JA-2008-042

9. SPONSORING / MONITORING AGENCY NAME(S) AND ADDRESS(ES)

Air Force Research Laboratory (AFMC)
AFRL/RZS
5 Pollux Drive
Edwards AFB CA 93524-7048

10. SPONSOR/MONITOR'S ACRONYM(S)

11. SPONSOR/MONITOR'S NUMBER(S)
AFRL-RZ-ED-JA-2008-042

12. DISTRIBUTION / AVAILABILITY STATEMENT

Approved for public release; distribution unlimited (PA #08159A).

13. SUPPLEMENTARY NOTES
For publication in Computer Physics Communications.

14. ABSTRACT

In this paper a second order discontinuous Galerkin method for the Hall MHD equations including diamagnetic drift is developed. The equations are formulated in gas dynamic conservative form and tested on the Brio and Wu MHD shock as well as the GEM challenge magnetic reconnection problem. Solutions compare well with previously published results. The algorithm is easily extended to general geometries.

15. SUBJECT TERMS

16. SECURITY CLASSIFICATION OF:			17. LIMITATION OF ABSTRACT	18. NUMBER OF PAGES	19a. NAME OF RESPONSIBLE PERSON
					Dr. Jean-Luc Cambier
a. REPORT	b. ABSTRACT	c. THIS PAGE	SAR	21	19b. TELEPHONE NUMBER *(include area code)*
Unclassified	**Unclassified**	**Unclassified**			N/A

A Numerical Approach to Solving the Hall MHD Equations Including Diamagnetic Drift (PREPRINT)

J. Loverich*

Advatech Pacific

J-L. Cambier

AFRL Edwards

Abstract

In this paper a second order discontinuous Galerkin method for the Hall MHD equations including diamagnetic drift is developed. The equations are formulated in gas dynamic conservative form and tested on the Brio and Wu MHD shock as well as the GEM challenge magnetic reconnection problem. Solutions compare well with previously published results. The algorithm is easily extended to general geometries.

[0] Distribution A: Public Release, Distribution Unlimited

*Electronic address: loverich@txcorp.com

I. INTRODUCTION

In situations where the full two-fluid plasma system(23) is difficult to solve, near the MHD limit for example where the Hall parameter is small, a simpler approach is to solve the two-temperature Hall MHD model with diamagnetic drift. This model eliminates the displacement current as well as charge separation and the electron cyclotron frequency while still capturing many two-fluid effects. Hall MHD has been studied by many authors and several algorithms have been developed (3; 11; 13; 14). The discontinuous Galerkin technique has been applied to many plasma systems (16; 17; 20; 24) and the technique is discussed in great detail in general terms in the textbook by Hesthaven and Warburton (12). James Wiley of University of Texas at Austin also investigated DG method for the Hall MHD system though that work remains un-published. This work is unique in that the discontinuous Galerkin method is used and the algorithm is developed from the Hall MHD equations in gas dynamic conservative form. It is believed that this form is appropriate because the magnetic field and ion fluid decouple in regimes where the Hall term is important and therefore shocks appear that obey the ion jump conditions only. Currently these results are restricted to second order spatial accuracy and 3rd or 4th order temporal accuracy.

II. SYSTEM OF EQUATIONS

The model is derived by assuming that the speed of light is large in comparison to other speeds in the system. Quasi-neutrality is assumed, so that only one continuity equation is required,

$$\frac{\partial \rho_i}{\partial t} + \nabla \cdot [\rho_i \, U_i] = 0 \,, \tag{1}$$

Along with a momentum equation for the ions,

$$\frac{\partial \rho_i \, U_i}{\partial t} + \nabla \cdot [\rho_i \, U_i \, U_i + P_i] = n_i \, q_i \, E + J_i \times B \,, \tag{2}$$

an ion energy equation,

$$\frac{\partial e_i}{\partial t} + \nabla \cdot [U_i \, (e_i + P_i)] = J_i \cdot E \,, \tag{3}$$

where e_i is the ion kinetic energy + internal energy, and an electron energy equation,

$$\frac{\partial e_e}{\partial t} + \nabla \cdot [U_e \, (e_e + P_e)] = J_e \cdot E \, . \tag{4}$$

where e_e is the electron kinetic energy + the electron internal energy - however, electron kinetic energy is zero because the electron mass is set to zero. The species currents are J_α where $\alpha = e, i$ for the electrons and ions respectively. The ideal gas equation of state is used, therefore $P_i = n_i \, k \, T_i$ and $P_e = n_e \, k \, T_e$. The completeness of the system requires a momentum equation for the electron fluid. Since the electrons are assumed massless the convective derivative is set to zero and we are left with pressure and Lorentz forces. The reduced electron momentum equation or Ohm's law, is given by

$$\Psi = n_e \, q_e \, E = -J_e \times B + \nabla \, P_e \, . \tag{5}$$

The magnetic field equation is also included

$$\frac{\partial B}{\partial t} + \nabla \times E = 0 \, . \tag{6}$$

In this paper divergence cleaning is accomplished using the hyperbolic divergence cleaning method as suggested in (9). Using this formulation an additional equation is added and the magnetic field equation is modified, thus

$$\frac{\partial B}{\partial t} + \nabla \times E + \nabla \phi = 0 \, . \tag{7}$$

and

$$\frac{\partial \phi}{\partial t} + \Gamma^2 \nabla \cdot B = -\zeta \phi \, . \tag{8}$$

The modified magnetic field equation adds the divergence wave to the system which propagates divergence errors out of the domain at speed Γ while simultaneously damping them. A linear wave analysis shows that this divergence wave does not couple to the plasma and therefore does not modify any other plasma wave.

III. DISPERSION RELATION

For complicated systems the wave systems may contain dispersive waves where the frequency ω depends on wave number k in a non-linear fashion. Hall MHD in particular, admits solutions where ω is quadratic in k. A careful analysis of dispersion relations is often necessary in order to properly determine time step restrictions. The following can be said about Hall MHD,

The Hall MHD model produces the whistler wave in the case where the wave travels parallel to the magnetic field

$$w = \frac{B_0}{2q\,n_0\,\mu_0}k^2 + \frac{B_0\sqrt{4\,n_0\,m_i\,\mu_0\,q^2 + k^2\,m_i^2}}{2\,q\,m_i\,n_0\,\mu_0}\,k\,. \tag{9}$$

Note that this can be written

$$w = \frac{1}{2}\omega_{c\,i}\,d_i^2\,k^2 + \sqrt{V_A^2k^2 + \frac{1}{2}\,\omega_{ci}^2\,d_i^4\,k^4}\,, \tag{10}$$

where $d_i = \frac{c}{\omega_{p\,i}} = c\sqrt{\frac{m_i\,\epsilon_0}{n_0\,q^2}}$ is the ion inertial length or ion skin depth, $V_A = \frac{B_0}{\sqrt{n_0 m_i\,\mu_0}}$ is the Alfven wave speed and $V_w = \omega_{c\,i}d_i^2 = \frac{B_0}{q\,n_0\,\mu_0}$ is the whistler coefficient. The whistler wave becomes,

$$\omega = \omega_{c\,i}\,d_i^2\,k^2 \tag{11}$$

for sufficiently large k. The importance of the Hall term (and hence the whistler wave) can be determined by the ratio of the contributions of the quadratic and linear terms in the whistler wave dispersion relation, thus, the whistler wave is important when,

$$\frac{V_w}{V_A}k = d_i k \gtrapprox 1\,. \tag{12}$$

This condition implies that the Hall term is important for frequencies where $\omega \gtrapprox \omega_{ci}$ and for wavelengths $L = \frac{2\pi}{k}$ where $L \lessapprox d_i$.

For small wave numbers the whistler wave becomes the Alfven wave and ω varies linearly with k. In the limit of long wave lengths ω varies quadratically with k, thus we have traditional convection combined with dispersive convection. This sort of consideration suggests

the following system as a simple model for the ideal Hall MHD system

$$\frac{\partial u}{\partial t} = \delta_1 \frac{\partial u}{\partial x} - i\,\delta_2 \frac{\partial^2 u}{\partial x^2}\,. \tag{13}$$

If the non-dispersive advective term is ignored we simply have,

$$\frac{\partial u}{\partial t} = -i\,\delta_2 \frac{\partial^2 u}{\partial x^2}\,. \tag{14}$$

which is equivalent to the Schrodinger equation. Fortunately, numerical solutions to the Schrodinger equation have been studied for decades, see for example (4), and basic stable schemes can be borrowed from previous work.

In the case where the wave travels perpendicular to the magnetic field the dispersion relation produces the magnetosonic wave

$$w = \pm\, k \sqrt{\frac{B_0^2 + P_0 \gamma \mu_0}{m_i\, n_0\, \mu_0}} \tag{15}$$

which is non-dispersive and linear in k.

A. Time Step Restrictions

Using an explicit code the following time step restrictions are suggested. First of all the magnetosonic wave V_m should be resolved, thus

$$\Delta t < \frac{\Delta x}{|U| + V_m} \tag{16}$$

From the whistler wave dispersion relation the maximum time step should be

$$\Delta t < \frac{\Delta x^2}{V_w} \tag{17}$$

In general then,

$$\Delta t < \min\left[\frac{\Delta x}{|U| + V_m}, \frac{\Delta x^2}{V_w}\right] \tag{18}$$

Drift waves also exist in the Hall MHD system and the actual time step may be more restrictive. Huba discusses this in more detail in (14). For many problems the Whistler

wave dominates and taking a time step based on its value is frequently adequate.

IV. NUMERICAL APPROACH

The numerical approach used is the discontinuous Galerkin method. The discontinuous Galerkin method can be considered an extension of finite volume methods or a finite element method where the solution can be discontinuous at nodes. The technique is described for hyperbolic systems in (5–8). The method is explicit and does not require the solution of a global mass matrix at each time step.

Start by defining n auxiliary variables. In the case of Hall MHD with diamagnetic drift, n is 2. These auxiliary variables are written generically as,

$$v_1 = \nabla \cdot w_1 \left(q, v_1 \right) + \psi_1 \left(q, v_1, \mathbf{r} \right) . \tag{19}$$

$$v_2 = \nabla \cdot w_2 \left(q, v_2, v_1 \right) + \psi_2 \left(q, v_2, v_1, \mathbf{r} \right) . \tag{20}$$

and finally,

$$v_n = \nabla \cdot w_n \left(q, v_{n-1}, ..., v_1 \right) + \psi_n \left(q, v_{n-1}, ..., v_1, \mathbf{r} \right) . \tag{21}$$

The q are "conserved" variables, the v are auxiliary variables, the w are flux functions and the ψ are terms that only depend on algebraic combinations of q, v, and $\mathbf{r}$ where $\mathbf{r}$ is a vector position. Using the above formulation the Hall MHD system can be described. The auxiliary variables for the Hall MHD system are defined as,

$$v_1 = J = \frac{1}{\mu_0} \nabla \times B \tag{22}$$

and

$$v_2 = \Psi = n_e \, q_e \, E = - \left(J - J_i \right) \times B + \nabla \, P_e \, . \tag{23}$$

In addition, take the balance law,

$$\frac{\partial \, q}{\partial \, t} + \nabla \cdot f \left(q, v_n, ..., v_2, v_1 \right) = \psi \left(q, v_n, ..., v_2, v_1, \mathbf{r} \right) \tag{24}$$

where f is a flux function.

The balance law represents each of the equations with time derivatives in them in the Hall MHD system. The approach is to solve for the auxiliary variables one after another, using the solution v_{n-1} to solve for v_n, then substitute these solution into the balance law.

Using quadrilateral elements, Legendre polynomials are used as basis function and each of the variables v_n and q_n are represented as a linear combination of Legendre polynomials. Therefore if the basis set is h_r, where h_r is the rth Legendre polynomial, then the variables are represented as,

$$v_n = \sum_{r=0}^{p-1} \alpha_{n\,r} h_r \,, \tag{25}$$

$$q_n = \sum_{r=0}^{p-1} \beta_{n\,r} h_r \,, \tag{26}$$

where p is the number of basis functions in the expansion. In 1-D, p corresponds to the order of accuracy of the scheme. In 2-D for a strictly n^{th} order scheme $p = \frac{1}{2}(n+1)\,n$ where 2D Legendre polynomials are used as the bases. In equation (25) $\alpha_{n\,r}$ represents the r^{th} basis coefficient of the n^{th} auxiliary variable and in equation (26) $\beta_{n\,r}$ represents the r^{th} coefficient of the n^{th} "conserved" variable. For a system of one auxiliary variable and one conserved variable you can eliminate the subscript n to see that each auxiliary variable and each conserved variable is simply a sum of Legendre polynomials. These same basis functions are used to expand the system of equations. First the auxiliary variables are considered. Multiply the equation (21) by the basis function set h_r and integrate over the volume to get,

$$\int_\Omega v_n\, h_r\, d\Omega = \int_\Omega \nabla \cdot w_n\left(q, v_{n-1}, ..., v_1\right)\, h_r\, d\Omega + \int_\Omega \psi_n\left(q, v_{n-1}, ..., v_1, \mathbf{r}\right)\, h_r\, d\Omega \tag{27}$$

Integration by parts is applied to the derivative to yield,

$$\begin{aligned}\int_\Omega v_n\, h_r\, d\Omega = &\int_{\partial\Omega} \left[w_n\left(q, v_{n-1}, ..., v_1\right)\, h_r\right] \cdot \bar{n}\, d\partial\Omega - \\ &\int_\Omega w_n\left(q, v_{n-1}, ..., v_1\right) \cdot \nabla\, h_r\, d\Omega + \int_\Omega \psi_n\left(q, v_{n-1}, ..., v_1, \mathbf{r}\right)\, h_r\, d\Omega = T_{n\,r}\end{aligned} \tag{28}$$

Substituting the definition of v_n (25) into the first term of equation (28), the following result is obtained

$$\int_\Omega v_n\, h_r\, d\Omega = \sum_{g=0}^{p-1} \alpha_{n\,g} \int_\Omega h_g\, h_r\, d\Omega = \sum_{g=0}^{p-1} \alpha_{n\,g}\, A_{g\,r} \tag{29}$$

so that

$$A_{g\,r} = \int_{\Omega} h_g \, h_r \, d\Omega \, . \tag{30}$$

On regular grid, $A_{g\,r}$ is diagonal since the basis functions are orthogonal. Now the coefficients $\alpha_{n\,g}$ can be calculated based on a numerical solution to the right hand side of (28), so that

$$\alpha_{n\,g} = T_{n\,r}[A_{g\,r}]^{-1} \tag{31}$$

$A_{g\,r}$ is a square matrix of size $p \times p$, $\alpha_{n\,g}$ is a matrix of size $m \times p$ where m is the number of auxiliary variables in the system and $T_{n\,r}$ is a $m \times p$ matrix. The right hand side is solved by numerically integrating the integrals at each time step. $A_{g\,r}$ is evaluated at the beginning of the simulation. The only derivatives that remain are on the basis function h_r and those can be calculated either analytically in the case of cartesian coordinates or numerically for general geometries. The terms that remain $w_n \left(q, v_{n-1}, ..., v_1\right)$ and $\psi_n \left(q, v_{n-1}, ..., v_1, \mathbf{r}\right)$ are algebraic function of q and v_n which are known (as a result of the basis function expansion of equations (25) and (26)) at all points in space. Gaussian quadrature is performed to approximate the integrals. For a second order method in 1D a 2 point gaussian quadrature is performed. In general in n dimensions a p^n point gaussian quadrature is performed for an order p accurate solution.

The balance laws are solved in a virtually identical manner except a time derivative must also be evaluated, for completeness, start with the balance law multiplied by the basis function set h_r.

$$\int_{\Omega} \frac{\partial \, q_n}{\partial \, t} \, h_r \, d\Omega + \int_{\Omega} \nabla \cdot f \left(q, v_1, v_2, ..., v_n\right) \, h_r \, d\Omega = \int_{\Omega} \psi \left(q, v_n, ..., v_2, v_1, \mathbf{r}\right) \, h_r \, d\Omega \, . \tag{32}$$

move the second term to the right hand side and expand the derivative using integration by parts

$$\begin{aligned} \int_{\Omega} \frac{\partial \, q_n}{\partial \, t} \, h_r \, d\Omega = & - \int_{\partial\Omega} \left[f \left(q, v_n, ..., v_2, v_1\right) \, h_r\right] \cdot \bar{n} \, d\partial\Omega + \\ & \int_{\Omega} f \left(q, v_n, ..., v_2, v_1\right) \cdot \, \nabla \, h_r \, d\Omega + \int_{\Omega} \psi \left(q, v_n, ..., v_2, v_1, \mathbf{r}\right) \, h_r \, d\Omega \, = Y_{n\,r} \end{aligned} \tag{33}$$

The definition of q is substituted into the first term so that the first term becomes

$$\int_\Omega \frac{\partial\, q_n}{\partial\, t}\, h_r\, d\Omega = \sum_{g=0}^{p-1} \frac{\partial \beta_{n\,g}}{\partial t} \int_\Omega h_g\, h_r\, d\Omega = \sum_{g=0}^{p-1} \frac{\partial \beta_{n\,g}}{\partial t}\, A^{g\,r}\,. \tag{34}$$

This gives us equations for the time derivative of $\beta_{n\,g}$

$$\frac{\partial \beta_{n\,g}}{\partial t} = Y_{n\,r}\,[A_{g\,r}]^{-1}. \tag{35}$$

Once the right hand side of equation (35) is calculated numerically, the $\beta_{n\,g}$ can be calculated using a standard second order Runge-Kutta technique. Note that $\beta_{n\,g}$ is a $m \times p$ matrix and so is $Y_{n\,r}$. Notice that the right hand side of equation (33) is identical in form to (28). The right hand side of (33) is therefore calculated in an identical manner.

A. Numerical Fluxes

One important issue in applying discontinuous Galerkin methods is the evaluation of the numerical flux. At boundary interfaces the flux is undefined because the solution is generally discontinuous at that point. A simple flux, known as the local Lax Friedrichs flux can be used on the conserved variables, in this case

$$\tilde{F}_{i+1/2} = \frac{1}{2}\left(F_i^+ + F_{i+1}^-\right) - \frac{1}{2}|\lambda|\left(q_{i+1}^- - q_i^+\right) \tag{36}$$

in general, for auxiliary variables this same flux can be used, but it needs to be modified by the factor Δt, namely

$$\tilde{F}_{i+1/2} = \frac{1}{2}\left(F_i^+ + F_{i+1}^-\right) - \frac{1}{2}\Delta t|\lambda|\left(q_{i+1}^- - q_i^+\right) \tag{37}$$

Choice of fluxes for diffusive systems are discussed in (15) and flux functions for the Schrodinger equation are discussed in (19). Both papers indicate that centered fluxes will be stable, the added dissipation may help in avoiding negative pressures in certain situations.

V. RESULTS

A. Brio and Wu Shock

The Brio and Wu shock problem was recently extended to systems with finite ion inertial length effects in the following works (10; 16; 23) in the framework of the two-fluid plasma system. These same simulations can be run using Hall MHD with diamagnetic drift. The results that follow are Hall MHD solutions to these two-fluid shock problems.

Parameters used are $q_i = 10$, $q_e = -10$, and $\epsilon_0 = 1$, $\mu_0 = 1$, $c = 1$, $\gamma_e = \gamma_i = \frac{5}{3}$, $m_i = 1$. The initial conditions are given by $P_e = P_i = 0.5 \times 10^{-4}$, $n_e = n_i = 1.0$ and $B = (7.5 \times 10^{-3}, 1.0 \times 10^{-2}, 0)$ on the left half of the domain. On the right half of the domain the $P_e = P_i = 0.5 \times 10^{-5}$, $n_e = n_i = 0.125$ and $B = (7.5 \times 10^{-3}, -1.0 \times 10^{-2}, 0)$ while $U_e = U_i = E = 0$ everywhere.

Figures 1,2 and 3 show the Brio and Wu shock solution with $r_{g\,i} = 1/10$, $r_{g\,i} = 1/100$ and $r_{g\,i} = 1/1000$ respectively where $r_{g\imath}$ is the ion gyroradius given the initial conditions on the left hand side of the shock. The ion gyroradius is calculated as $v_{th\,i}/\omega_{c\,i}$ where $v_{th\,i}$ is the ion thermal velocity and $\omega_{c\,i} = \frac{q_i|B|}{m_i}$. Solutions are quite similar to those calculated previously using the two-fluid equations(10).

The two-fluid results are virtually identical to the Hall MHD results so it's tempting to suggest that Hall MHD should be used in the vast majority of cases because the physics is simpler. Difference only begin to appear at the Debye length. In regimes where the speed of light is high compared to fluid speeds the speed of light can be artificially reduced in the full two-fluid system. The reduced speed of light and electron inertia act to provide numerical limits for dispersive waves thus reducing the stiffness of the system compared to Hall MHD. The displacement current and electron inertia can be thought of as numerical parameters that would reduce the stiffness of the Hall MHD system just as artificial viscosity is often used to stabilize numerical solutions to purely hyperbolic otherwise non viscous system. The full two-fluid system can thus be thought of as the Hall MHD system with numerical terms that limit the stiffness of Hall MHD. When actually running the simulations in the regime where $r_{g\,i} \approx 1/10$ the domain or larger, the full two-fluid simulations complete considerably faster than the Hall MHD simulations. At the other extreme, where $r_{g\imath} \approx 1/1000$ the Hall MHD simulations complete considerably faster than the two-fluid simulations provided that

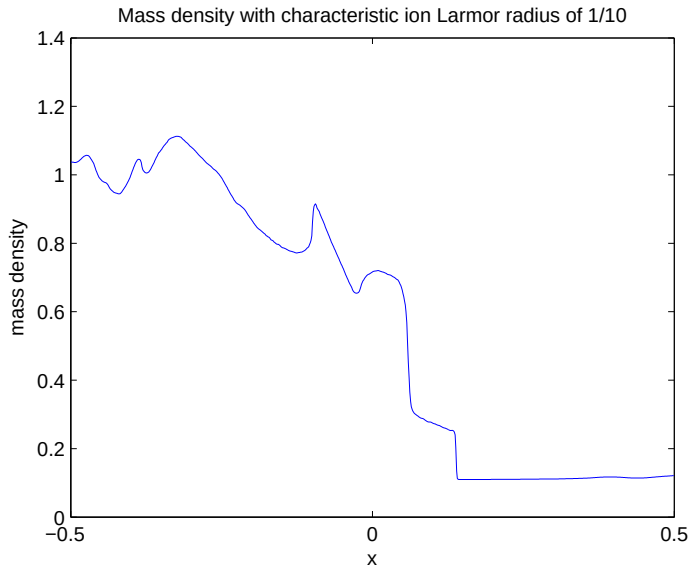

FIG. 1 Hall MHD solution to the Brio and Wu shock problem with characteristic ion Larmor radius of 1/10. The Hall MHD solution agrees quite well with published two-fluid solutions. In this case the obvious differences are Debye length oscillations which occur at the shock (and elsewhere) in the two-fluid solution.

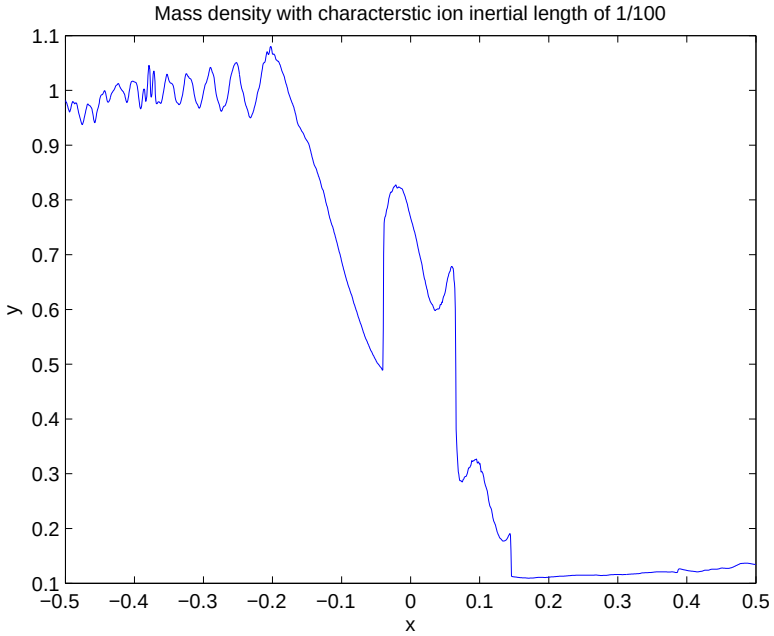

FIG. 2 Hall MHD solution to the Brio and Wu shock problem with characteristic ion inertial length 1/100. The Hall MHD solution agrees quite well with published two-fluid solutions. Major differences include the large oscillations on the left of the shock. These oscillation also appear in the two-fluid solutions when sufficiently small time step are taken.

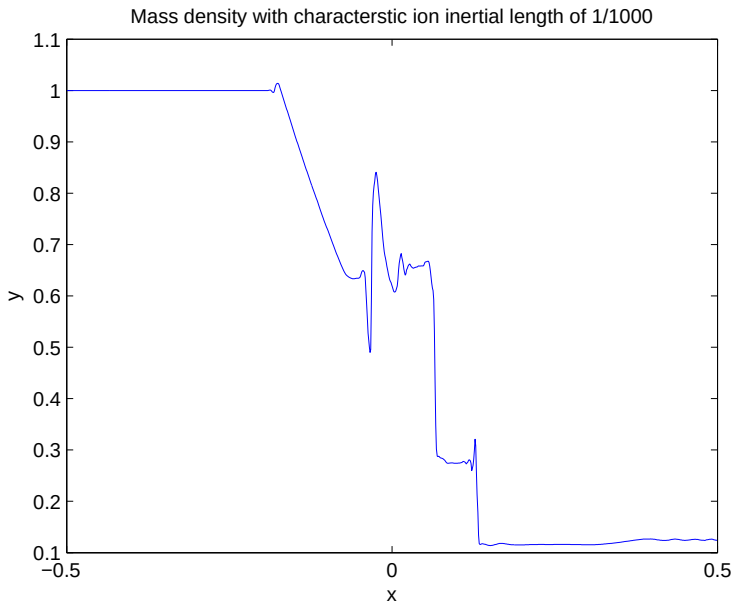

FIG. 3 Hall MHD solution to the Brio and Wu shock problem with characteristic ion inertial length 1/1000. The solution agrees remarkably well with published two-fluid solutions. In this regime the two-fluid solution is particularly difficult to solve due to the stiffness of the system. The Hall MHD solution on the other hand is quite simple because the solution is a small perturbation from the MHD solution.

r_{gi} is not well resolved. Moving towards the MHD limit where the whistler wave is not well resolved, solving the Hall system is still computationally efficient, however as resolution increases, the whistler wave speed increases and a technique that limits the whistler wave speed is desirable. The two-fluid model becomes computationally inefficient near the MHD limit because cyclotron and plasma frequency time scales must be resolved along with Debye length spatial scales so that much larger computational grids are necessary than are required for Hall MHD where these same time and spatial scales do not need to be resolved.

Relative computational times can be estimated by looking at the waves involved. The full two-fluid model can be solved in roughly the same manner as the Hall MHD system, so one step of the Hall MHD algorithm takes about as long as one step of a full two-fluid algorithm. Therefore, simulation time depends on the necessary spatial resolution and time step restriction. In full two-fluid $\Delta t = \Delta x/c$ where c is the speed of light. For Hall MHD the fastest wave is given approximately by $\omega_{ci} d_i^2/\Delta x$ so that $\Delta t = \frac{\Delta x^2}{\omega_{ci} d_i^2}$. Computational effort required for each system is given roughly by $\frac{1}{\Delta x \Delta t}$ so that the ratio of computational

effort (time) is

$$\frac{E_{TF}}{E_{Hall}} \approx \frac{c\,\Delta x}{\omega_{c\,i} d_i^2} \tag{38}$$

where E_{TF} is the computation time required to solve the full two-fluid system at the given resolution and E_{Hall} is the computational time required to solve the Hall MHD system at the same resolution. It is clear that as resolution increases, i.e. Δx decreases, the full two-fluid system requires less time to solve relative to the Hall MHD system.

Ultimately one could argue that implicit schemes are of greater importance and time constraints are less dependent on grid resolution in that case, however the above also suggest that at high resolution the full two-fluid system is less stiff than the Hall MHD system and faster convergence might be observed using implicit methods on the full two-fluid system than on the Hall MHD system.

B. Magnetic Reconnection

Magnetic reconnection is an important test of Hall MHD codes and has become a standard benchmark of Hall MHD and Two-Fluid codes. The following results illustrate Hall reconnection with results compared to solutions computed using other methods. A good reference for collisionless reconnection can be found in (2), and in the GEM challenge papers (21; 22).

The GEM challenge magnetic reconnection problem is non-dimensionalized as in (1) where lengths are normalized by the ion inertial length $d = c/w_{pi} = c\left(\frac{e^2\,n_0}{\epsilon_0\,m_i}\right)^{-\frac{1}{2}}$ time is non-dimensionalized by the ion-cyclotron time $\frac{m_i}{e\,B_0}$ where B_0 is the magnetic field at infinity. The velocities are normalized by the Alfven velocity $V_a = \left(\frac{B_0^2}{\mu_0\,m_i\,n_0}\right)^{\frac{1}{2}}$. Finally current density is non-dimensionalized by $J_0 = \frac{B_0\,w_{pi}}{\mu_0\,c}$ and E by $E_0 = V_a\,B_0$. The domain is $(-6.4\,d, 6.4\,d)$ and the simulation is run out to $40/w_{ci}$. Conducting walls are used on the y boundaries and periodic boundaries are used on the x boundaries. $\lambda = 0.5\,d$ and the specific heat ratio $\gamma = \frac{5}{3}$. The initial number densities are given by,

$$n = n_0\left(\frac{1}{5} + \operatorname{sech}^2\left(\frac{y}{\lambda}\right)\right)\,. \tag{39}$$

The electron and ion temperatures differ slightly from the GEM challenge problem in that the electron and ion temperatures are equal, this gives the following electron pressure, P_e,

$$P_e = \frac{3}{12\mu_0}B_0^2\,\frac{n_e}{n_0} \tag{40}$$

and ion pressure P_i

$$P_i = \frac{3}{12\mu_0}B_0^2\,\frac{n_i}{n_0}. \tag{41}$$

The electron and ion pressure balance the magnetic field which is given by

$$B_x = B_0\tanh\left(\frac{y}{\lambda}\right) + \frac{B_0}{10}\frac{\pi}{L_x}\cos\left(\frac{2\pi\,x}{L_x}\right)\sin\left(\frac{\pi\,y}{L_y}\right) \tag{42}$$

$$B_y = \frac{B_0}{10}\left(\frac{2\pi}{L_x}\right)\sin\left(\frac{2\pi\,x}{L_x}\right)\cos\left(\frac{\pi\,y}{L_y}\right) \tag{43}$$

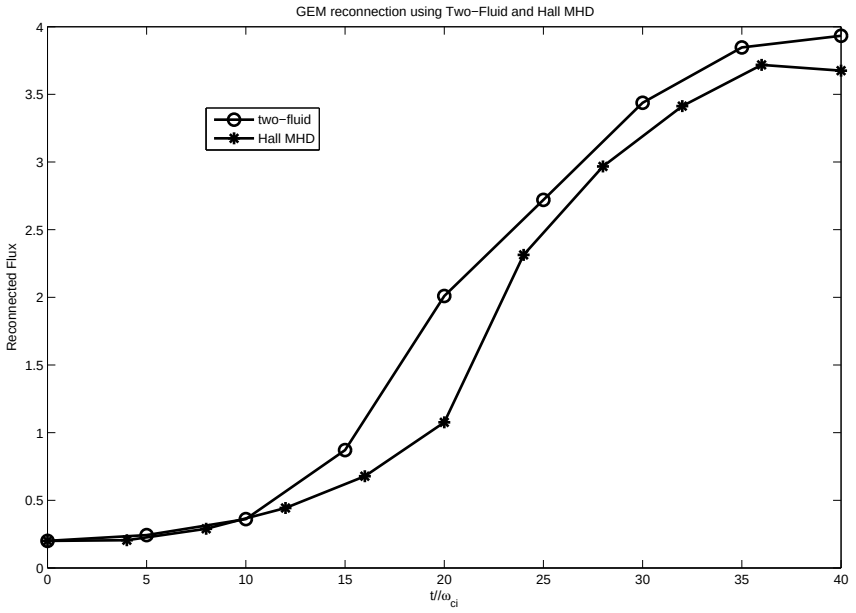

FIG. 4 Plots of reconnected flux calculated using the full two-fluid system and the Hall MHD system discussed in this paper.

The magnetic field is in equilibrium with with the current J,

$$J_{ze} = \frac{\mu_0 B_0}{\lambda} \operatorname{sech}^2\left(\frac{x}{\lambda}\right) . \tag{44}$$

However, for the Hall MHD system, J is calculated numerically from B so it is not necessary to set it as an initial condition.

Figure 4 shows the reconnected flux vs. time for the Hall MHD solution compared to the two-fluid solution calculated in (16). The reconnection rates agree fairly well as expected, both solutions produce fast reconnection. Figure 5 shows plots of total current using the Hall MHD code at time $t = 28/\omega_{ci}$. The Hall MHD solution shows much less structure than the two-fluid solution; this is likely a result of the neglect of electron inertia, the electron convective derivative in particular, which allows shear instabilities in the electron fluid in the two-fluid case.

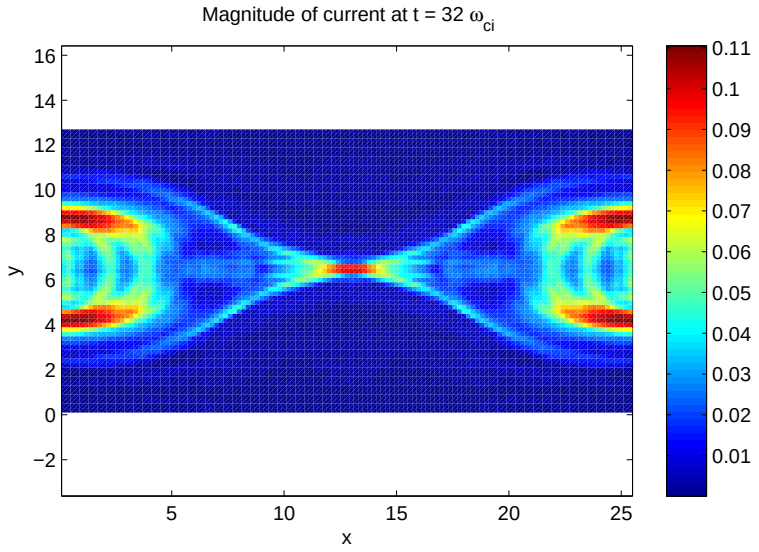

FIG. 5 A Low resolution simulation of Hall reconnection. Growth rate is somewhat lower than expected for a high resolution simulation.

C. Axisymmetric Z-Pinch

The Z-pinch is a good test of the axisymmetric code. In this case a new benchmark is presented based on the Hall solution to the axisymmetric Z-pinch originally presented in (18) which used the full two-fluid model. The Hall solution is important because now the two techniques can be compared and differences in the two plasma models identified. Both Hall MHD and the full two-fluid model show the development of a fast instability on the scale of the ion inertial length d_i. In the Hall MHD solution shown in figure 6 the structure is a finer, this may be explained by the fact that in Hall MHD the electron mass is zero so electron inertia effects are ignored.

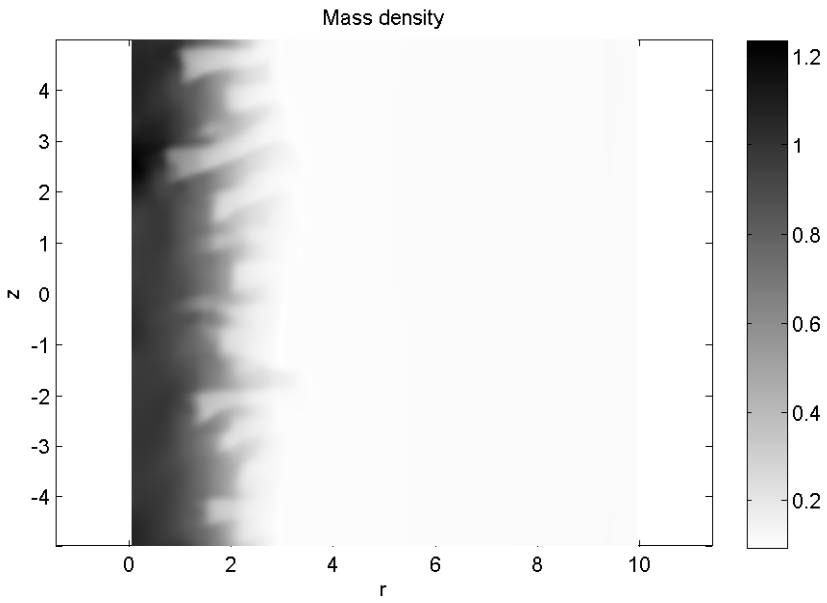

FIG. 6 Mass density of a Z-pinch where the axis are in units of ion Larmor radii. The solution shows the growth of a fast instability much like that in Figure 8 of (18) where the same initial conditions are used.

VI. CONCLUSION

A Hall MHD code including diamagnetic drift has been developed using the discontinuous Galerkin method. The technique is explicit and involves a straight forward application of the DG method. In principal this same algorithm can be extended to 3rd and higher order accuracy and can be applied to non-Cartesian grids. The simulations of Brio and Wu shock show good agreement with those performed using the full two-fluid model, however it has been observed that the full two-fluid model is actually achieves solutions faster than Hall MHD in regimes where the Hall parameter is large compared to the domain size. Simulations of magnetic reconnection agree with prior published results as do simulations of fast instabilities in Z-pinches.

References

[1] J. Birn and et al. Geospace environmental modeling (gem) magnetic reconnection challenge. *Journal of Geophysical Research*, 106(A3):3715–3719, 2001.

[2] D. Biskamp, E. Schwarz, and J.F. Drake. Two-fluid theory of collisionless magnetic reconnection. *Physics of Plasmas*, pages 1002–1009, 1997.

[3] L. Chacon and D.A. Knoll. A 2d high-beta hall mhd implicit nonlinear solver. *Journal of Computational Physics*, 188:573–592, 2003.

[4] Tony F. Chan, Ding Lee, and Longjun Shen. Stable explicit schemes for equations of the schrodinger type. *Siam Journal of Numerical Analysis*, 23(2):274–281, 1986.

[5] Bernardo Cockburn, Suchung Hou, and Chi-Wang Shu. The runge-kutta local projection discontinuous galerkin finite element method for conservation laws iv: Multidimensional case. *Mathematics of Computation*, 54:545–581, 1990.

[6] Bernardo Cockburn, San-Yih Lin, and Chi-Wang Shu. Tvb runge-kutta local projection discontinuous galerkin finite element method for conservation laws iii: One-dimensional systems. *Journal of Computational Physics*, 84:90–113, 1989.

[7] Bernardo Cockburn and Chi-Wang Shu. Tvb runge-kutta local projection discontinuous galerkin finite element method for conservation laws ii: General framework. *Mathematics of Computation*, 52:411–435, 1989.

[8] Bernardo Cockburn and Chi-Wang Shu. The runge-kutta discontinuous galerkin method for conservation laws v: Multidimensional systems. *Journal of Computational Physics*, 141:199–224, 1998.

[9] A. Dedner, F. Kemm, D. Kroner, T. Schnitzer, and M. Wesenberg. Hyperbolic divergence cleaning for the mhd equations. *Journal of Computational Physics*, 175:645–673, 2002.

[10] A. Hakim, J. Loverich, and U. Shumlak. A high resolution wave propagation scheme for ideal two-fluid plasma equations. *Journal of Computational Physics*, 2006.

[11] D.S. Harned and Z. Mikic. Accurate semi-implicit treatment of the hall effect in magnetohydrodynamic computations. *Journal of Computational Physics*, 83:1–15, 1989.

[12] Jan S. Heshaven and Tim Warburton. *Nodal Discontinuous Galerkin Methods, Algorithms, Analysis, and Applications*. Springer, New York, USA, 2008.

[13] Joseph D. Huba. Hall magnetohydrodynamics - a tutorial. In M. Scholer J. Buchner, C.T. Dunn, editor, *Space Plasma Simulation*, pages 166–192. Springer, 2003.

[14] Joseph D. Huba. Numerical methods: Ideal and hall mhd. 2005.

[15] Robert M. Kirby and George Em Karniadakis. Selecting the numerical flux in discontinuous galerkin methods for diffusion problems. *Journal of Scientific Computing*, 22 and 23:2094–2103, June 2005.

[16] J. Loverich. A discontinuous galerkin algorithms for the two-fluid plasma model with application to the z-pinch, 2005.

[17] J. Loverich and U. Shumlak. A discontinuous galerkin method for the full two-fluid plasma model. *Computer Physics Communications*, (169):251–255, 2005.

[18] J. Loverich and U. Shumlak. Nonlinear full two-fluid study of m=0 sausage instabilities in an axisymmetric z pinch. *Physics of Plasmas*, (13), 2006.

[19] Tiao Lu, Wei Cai, and Pingwen Zhang. Conservative local discontinuous galerkin methods for time dependent schrodinger equation. *Physics of Plasmas*, 2(1):78–84, 2005.

[20] A. Mangeney, F. Califano, C. Cavazzoni, and P. Travnicek. A numerical scheme for the integration of the vlasov-maxwell system of equations. *Journal of Computational Physics*, 179:495–538, 2002.

[21] A. Otto. Geospace environment modeling (gem) magnetic reconnection challenge: Mhd and hall mhd - constant and current dependent resistivity models. *Journal Of Geophysical Research*, 106:3751–3757, 2001.

[22] M. A. Shay, J. F. Drake, B. N. Rogers, and R. E. Denton. Alfvenic collisionless magnetic reconnection and the hall term. *Journal of Geophysical Research*, 106:3759–3772, 2001.

[23] U. Shumlak and J. Loverich. Approximate riemann solver for the two-fluid plasma model. *Journal of Computational Physics*, 187:620–638, 2003.

[24] T. C. Warburton and G. E. Karniadakis. A discontinuous galerkin method for the viscous mhd equations. *Journal of Computational Physics*, 152:608–641, 1999.